



Effect of silver–clay film thickness on some physical properties and permeability

Meysam Sattari Najaf Abadi

Department of Mechanics, Shahre Rey Branch, Islamic Azad University, Tehran, Iran.

ARTICLE INFO

Article history:

Received: 22 November 2012;

Received in revised form:

5 April 2013;

Accepted: 13 April 2013;

Keywords

Nano silver–clay films,
Thickness,
Physical properties and permeability.

ABSTRACT

In this study, the different film thicknesses of nano silver–clay films were prepared by varying volumes of the composite dispersion for casting. Effect of film thickness on thermal behavior, solid-state crystallinity, water uptake and erosion, and water vapor permeability of the nano composite films were investigated. The film thickness caused a small change in thermal behavior of the films when tested using DSC and TGA. The crystallinity of the thin films increased when compared with the thick films. Water uptake and erosion, water vapor permeation of the thick films were higher than those of the thin films. The results suggest that the evaporation rate of solvent in different volumes of the composite dispersion used in the preparation method could affect crystallinity of the film surface and film bulk of the nano composite films. This led to a change in water vapor permeability of the films.

© 2013 Elixir All rights reserved.

Introduction

There is increasing scientific and commercial interest in the development of nano structured thin films due to their outstanding properties relative to single-phase materials. Several reports on ceramic–metal nano composites films are found in the literature. Ceramic films possess ultrahigh hardness. However, this high hardness is usually accompanied by low some of properties.

These properties can cause failure of the film when applied on deformable substrates. On soft and deformable substrates vapour-deposited thin composite films represent a potential solution for appropriate coatings as has been demonstrated by bearing designers and polymer tribologists, (Li *et al.*, 2004), as well as in some biological applications (yu *et al.*, 2004). The silver–clay system can be a suitable model for the investigation of structure development in ceramic –metal nano composites and their structure-property relations.

Previous investigation of silver–clay films revealed the formation of metastable structures. Formation of amorphous silver–clay alloy was reported in (Reda *et al.*, 1982), while vapour deposited continuous silver–clay solid solution was forced to form at low deposition temperatures (sheng *et al.*, 2002). Dirks *et al.* studied the mechanical properties of vapour-deposited silver–clay thin films as a function of the chemical composition of the deposits. They revealed by XRD substantial solubility of both components (approx. 10 at. %) as well (Dirks *et al.*, 1984).

Summarising the literature data, we can see that compositionally (solid solution) and morphologically (amorphous) metastable structures can form in the silver–clay system. This can involve the possibility of the formation of nanostructured films as well.

The aim of present research was to survey the possibility of nanostructure formation in the silver–clay system and describe the physical properties and permeability property relations.

Methods and Materials

Materials

Low viscosity grade of sodium alginate (silver, viscosity of 2% solution at 23 °C: 270 cps) was purchased from Sigma Chemical Company (MO, USA). Clay (Veegu HV) was obtained from R.T. Vanderbilt Company, Inc. (Norwalk, CT, USA). Acetaminophen (ACT) and propranolol HCl (PPN) were purchased from Praporn Darsut Ltd. (Tehran, Iran). Other reagents used were of analytical grade and used as received.

Preparation of films

Films were prepared using casting/solvent evaporation technique, which have been previously reported (Pongjanyakul *et al.*, 2005b). Silver was dispersed in distilled water using homogenizer for 5 min, whereas clay (2 g) was prehydrated with hot water for 15 min.

The clay dispersion was mixed into the silver dispersion using homogenizer for 5 min, and was then adjusted the volume with distilled water to 200 ml. The silver–clay dispersion was kept for full hydration at room temperature overnight. Then, 100, 200 or 300 ml of the composite dispersion was poured onto plastic plate (15 cm×20 cm), allowed to evaporate at 50 °C, and the durations for drying were approximately 12, 24 or 36 h, respectively. The composite films were peeled off and kept in desiccators (40±2% RH). Moreover, the silver film without clay was also prepared by using 200 ml of 1% (w/v) silver dispersion and then the preparation was preceded as described above.

Properties of films

Thickness of films

Thickness of dry and wet films was measured in 10 places using microprocessor coating thickness gauge (Minitest 600B, ElektroPhysik, Germany). The dry films (4 cm×4 cm) were cut and placed on a control plate. The probe, which was connected with the measurement gauge and calibrated using a standard film, gently moved downward to touch on the film and the thickness of film was then measured. The films were subsequently placed in a small beaker containing 0.1M HCl, which was shaken occasionally in water bath at 37.0±0.5 °C.

The samples were taken and blotted to remove excess water. The thickness of wet films was immediately determined following the procedure mentioned above.

Scanning electron microscopic studies

Surface morphology and cross-section of films were observed using SEM. Samples were mounted onto stubs, sputter coated with gold in a vacuum evaporator, and photographed using scanning electron microscope (Jeol Model JSM-5800LV, Tokyo, Japan).

Differential scanning calorimetry (DSC)

DSC thermograms of samples were recorded using a differential scanning calorimeter (DSC822, Mettler Toledo, Switzerland). Each sample (2–3 mg) was accurately weighed into a 40 μ l aluminum pan without an aluminum cover. The measurements were performed over 30–350 $^{\circ}$ C at a heating rate of 10 $^{\circ}$ C/min.

Thermo gravimetric analysis (TGA)

TGA thermo grams of samples were measured using a thermo gravimetric analyzer (TGA/SDTA851, Mettler Toledo, Switzerland). Each sample (3–4 mg) was accurately weighed into a 150 μ l alumina oxide crucible. The measurements were conducted over the range of 30–800 $^{\circ}$ C at a heating rate of 10 $^{\circ}$ C/min.

Powder X-ray diffractometry

Powder X-ray diffraction measurements were performed on a powder X-ray diffractometer (Philips PW3710 mpd control, The Netherlands). The measurement conditions were a Cu radiation generated at 30 kV and 20mA as X-ray source, angular of 1–35 $^{\circ}$ (2 θ) and step angle of 0.02 $^{\circ}$ (2 θ)/s.

Water uptake and erosion of films

Water uptake and erosion of the films were carried out using gravimetric method. Films were weighed (W_0) and then soaked in 0.1M HCl that had been incubated at 37.0 \pm 0.5 $^{\circ}$ C and shaken occasionally. After a predetermined time interval, each film was withdrawn, blotted to remove excess water, immediately weighed (W_t), and then dried in a hot air oven at 50 $^{\circ}$ C to constant weight (W_d). The % water uptake and % erosion can be calculated from the following equation (Tuovinen et al., 2003):

$$\text{water uptake (\%)} = \left(\frac{W_t - W_d}{W_d} \right) \times 100$$

$$\text{erosion (\%)} = \left(\frac{W_0 - W_d}{W_0} \right) \times 100$$

Where W_0 , W_t and W_d are the original, wet and dry weight of the films, respectively.

Water vapor permeability of films

Water vapor permeation (WVP) across the films was studied following the method of Remu and Bodmeier (1997). Discs were punched from the films, placed on open 5ml glass vials containing 3.5 g silica gel beads and held in place with a screw lid having a 0.86 cm-diameter of test area (0.58 cm²). The vials were placed in desiccators containing a saturated aqueous sodium chloride solution (75% RH) (Nyqvist, 1983). The desiccators were kept in a room at 26.0 \pm 1.0 $^{\circ}$ C, 55 \pm 3% RH. The weight change was recorded periodically over 72 h. The WVP rate was obtained from the slope of relationship between the amount of water permeated and time. The WVP coefficient of the films was calculated using the following equation (Porter and Ridgway, 1982; Limmatvapirat et al., 2004):

$$\text{WVP coefficient} = \frac{Mh}{A \Delta P_v}$$

Where M is the WVP rate, h is the mean thickness of the film, A is the area of the exposed film, and ΔP_v is the vapor pressure difference.

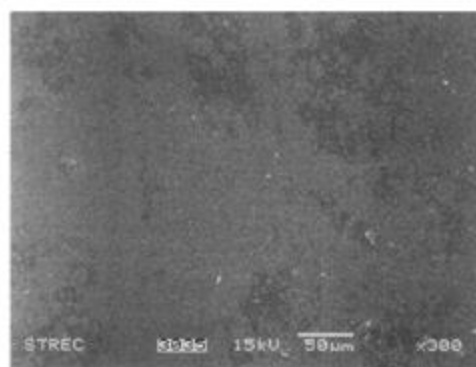
Statistical analysis

One-way analysis of variance (ANOVA) with the least significant difference (LSD) test for multiple comparisons was performed using SPSS program for MS Windows, release 11.5 (SPSS Inc., Chicago, IL) to assess statistical significance on mechanical property, water uptake, erosion and permeability data of the nano composite films. The significance of the difference was determined at 95% confident limit ($\alpha = 0.05$) and considered to be significant at a level of P less than 0.05.

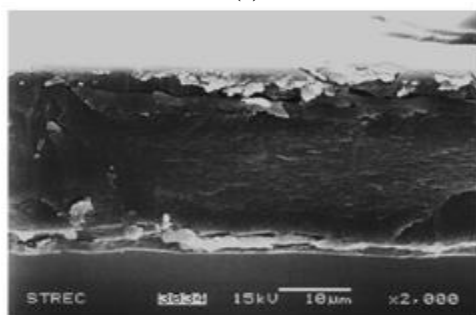
Results and discussion

Appearance and thickness of the films

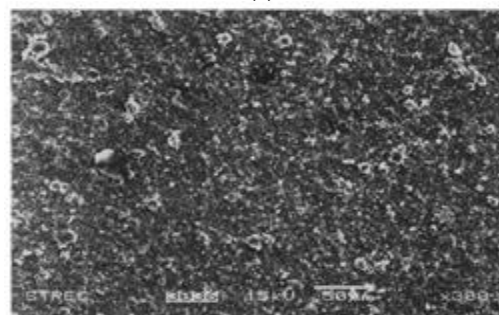
Silver and composite films were prepared using casting/solvent evaporation method. The transparent silver films were obtained, whereas incorporating clay gave opaque composite films. Surface morphology and internal structure of the silver films, which the film thickness was 45.3 \pm 1.8 μ m (n = 10), and the composite films were compared using SEM. Smooth surface and dense internal structures of the silver–clay film were observed (Fig. 1a and b). In contrast, the composite films had rough surface (Fig. 1c) and layer structure (Fig. 1d). This may be a result of interaction of silver with clay and recrystallization of clay (Pongjanyakul et al., 2005b).



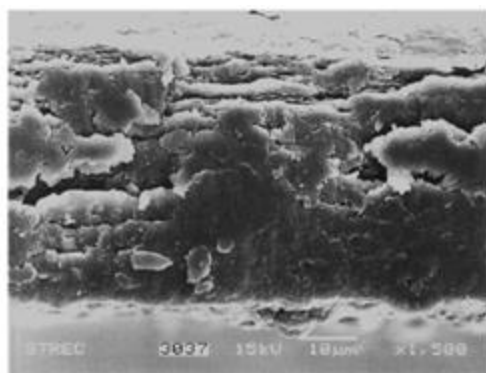
(a)



(b)



(c)



(d)

Fig. 1. Surface morphology and cross section of silver–clay film (a and b) and silver–clay nano composite film (c and d).

Although the composite films had looser matrix structure than the silver–clay films, but the composite films were stronger and more flexible than the silver–clay films (Pongjanyakul et al., 2005b). The thickness of the composite films is shown in Table 1. The dry and wet thickness of the composite films increased remarkably with increasing volume of the composite dispersion used.

The percentage of thickness increased after hydration in diluted HCl of all composite films was found to be 105–120% and significant effect of thickness on film hydration was not observed.

This indicated a swelling property of this composite film in acidic medium. Moreover, not only dry thickness but also wet thickness showed good linear correlation with solid content in composite dispersion used (Fig. 2). This suggested that the film thickness was directly dependent on solid content in composite dispersion.

Thermal behavior of the films

DSC thermo grams of the composite films are presented in Fig. 3. All films showed broad endothermic peaks around 50–70 °C, indicating a dehydration of water residue. The silver film showed an exothermic peak at about 220 °C and followed with an endothermic peak at about 224 °C, and an exothermic decomposition peak around 250 °C (Fig. 3b). The exothermic followed by the endothermic peak of the silver films may be attributable to recrystallization and a phase transition of c after heat induction (Pongjanyakul et al., 2005b).

These peaks shifted to lower temperature in the composite films. The increase in the thickness of the composite films caused these peaks shift to lower temperature. In addition, the exothermic decomposition peaks of the composite films showed lower intensity and higher temperature than that of the silver films. This decomposition peak of the composite films shifted to lower temperature when the film thickness was increased. The weight loss profile of the films at higher temperature was also studied using TGA.

Table 1. Dry and wet thickness of silver–clay nano composite films

Volume of silver–clay dispersion (ml)	Dry thickness ^a (µm)	Wet thickness ^a (µm)	Thickness increased after hydration ^b (%)
90	43.1 ± 1.3	67.8 ± 3.1	107.5
180	88.0 ± 8.1	177.4 ± 2.2	124.9
270	116.5 ± 3.0	233.8 ± 8.6	138.7

^a Data are the mean±S.D., *n* = 20. ^b ((Mean wet thickness–mean dry thickness)/mean dry thickness)×100.

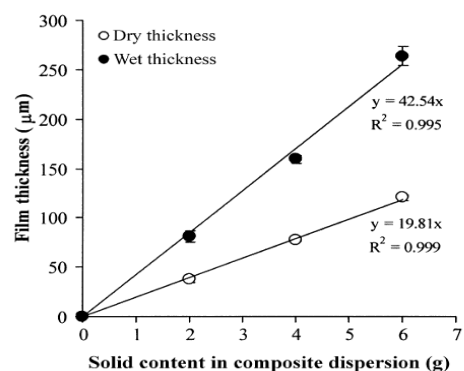


Fig. 2. Relationship between solid content in composite dispersion and film thickness of silver–clay nano composite films. Each point is the mean±S.D., *n* = 10.

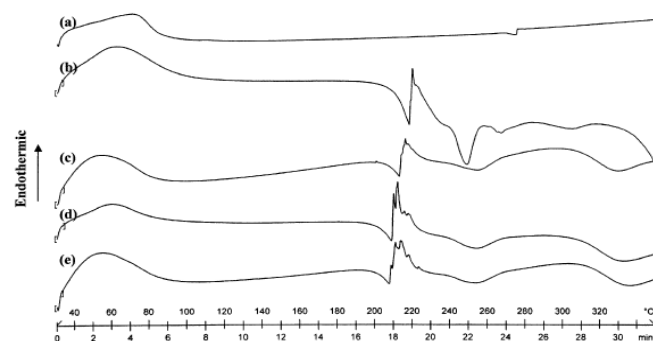


Fig. 3. DSC thermo grams of silver–clay (a), silver–clay film (b), and silver–clay nano composite films with different dry thickness of 43.1µm (c), 88.0µm (d) and 116.5µm (e).

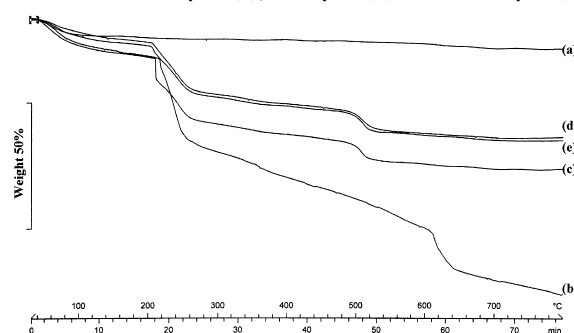


Fig. 4. Weight loss profiles of clay (a), silver–clay film (b), and silver–clay nano composite films with different dry thickness of 43.1µm (c), 88.0µm (d) and 116.5µm (e)

The loss of weight in the silver film at around 210–270 °C indicated a decomposition of silver–clay (Fig. 4b). At higher temperature the silver film showed a high weight loss at around 620–650 °C due to combustion of the residues. Clay showed a weight loss around 25–85 °C that correspond to the loss of surface and interlayer water. Moreover, the weight of clay slight reduced at temperature higher than 510 °C (Fig. 4a). This was due to dehydroxylation of the clay sheets (Grim, 1953). The total weight loss of clay was about 11% at 850 °C. In the case of the composite films, the weight loss at around 220–270 °C was a decomposition of the composite films, but the percent weight loss of the composite films was obviously lower than that of the silver–clay films. This was because of incorporation of clay into the films. However, the composite film with 43.1µm thickness gave higher wt% loss than that with 88.0 and 116.5µm thicknesses at this temperature (Fig. 4c and d). After that, the composite films had weight loss again at around 505–525 °C. It can be seen that the combustion of the residues of the composite

films occurred at lower temperature when compared with the silver films because the dehydroxylation of clay at this temperature may induce the combustion of the composite films. The thermal properties of the composite films found using DSC and TGA suggested that the film thickness affected thermal behavior of the composite films, indicating that the matrix structure of the films may be changed in the preparation process although the thickness of the composite films correlated with the solid content of dispersion used.

Crystallinity of the films

The crystallinity of the films was investigated using X-ray diffractometry. The silver film presented an amorphous form with a broad peak at 15° (2θ) (Fig. 5a). Clay powder showed a diffraction peak at approximately 8.1° (2θ), 18.9° (2θ), 23.0° (2θ), and 27.7° (2θ), indicating a crystalline form (Fig. 5b). When compared with clay and silver films, the composite films showed a different diffraction pattern with peaks at approximately 7.1 , 13.2 , 24.9 and 29.4° (2θ) (Fig. 5c and d), suggesting a change in crystallinity of the films. Similarity of XRD patterns of the composite films with various thicknesses was found. The basal spacing peak at 8° (2θ) of clay, represented the thickness of silicate layer (1.1 nm) (Darder et al., 2003; Wang et al., 2005), did not change in the composite films but increased in intensity, indicating that clay could form higher crystallinity by reaggregation of silicate layers during drying process (Lagaly, 1999). However, it can be observed that the basal spacing peak of the thinnest film presented stronger intensity than those of the thicker films, resulting in a higher crystallinity of the films.

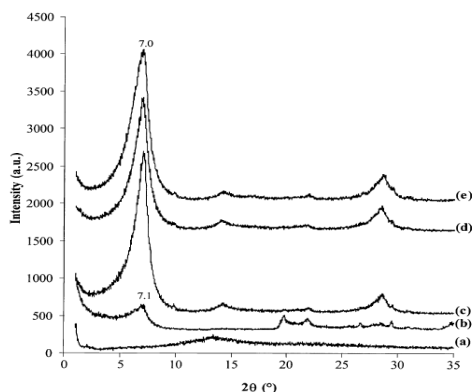


Fig. 5. PXRD patterns of clay (a), silver-clay film (b), and silver-clay nano composite films with different dry thickness of $43.1\mu\text{m}$ (c), $88.0\mu\text{m}$ (d) and $116.5\mu\text{m}$ (e).

The film thickness could affect crystallinity of the films due to the different condition of drying process. Jansson and Thuvander (2004) suggested that fast water evaporation in case of the thin films caused a limitation of molecular movement in the film, whereas slower water evaporation provided enough time for molecules to have relaxation. Since the thick films were exposed to a greater degree of water for a longer time, the crystallinity of the thick films were expected to be higher than the thin films. This expectation was not in agreement with the findings in this study. It can be explained that the fast evaporation of water in the composite dispersion might induce rapid reaggregation of clay, although clay could interact with silver in the composite dispersions. This might lead to higher crystallinity of the thinner films.

Water uptake and erosion of the films

The percent water uptake in 0.1M HCl of the films is shown in Fig. 6a. The water uptake of the thinnest films reached

equilibrium in 10 min, whereas the thicker films used a longer time (30 min). A faster water uptake was found in the thinnest film.

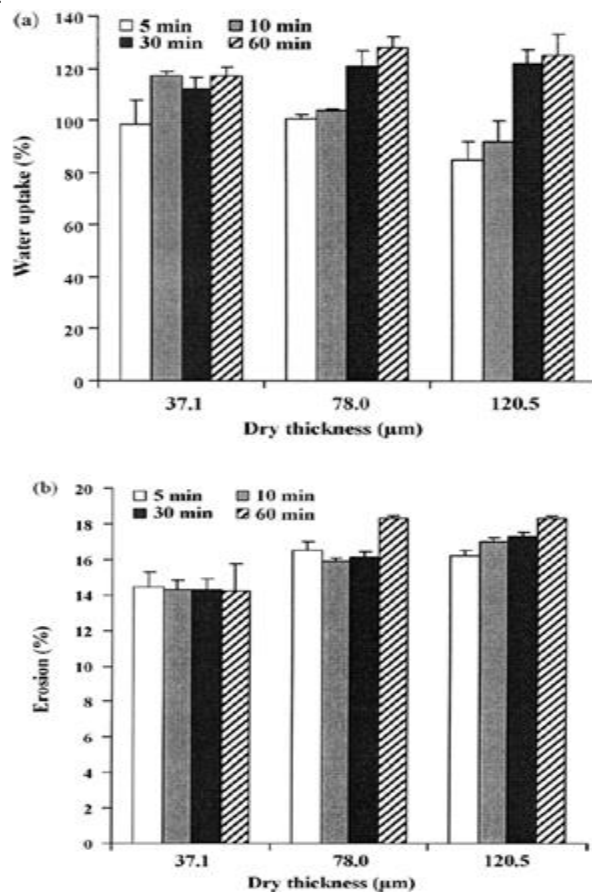


Fig. 6. Effect of dry thickness of nano composite films on water uptake (a) and erosion (b) in 0.1M HCl. Each bar is the mean \pm S.D., n=10

The thicker films (88.0 and $116.5\mu\text{m}$) provided statistically higher water uptake at 60 min ($P < 0.05$) than the thinnest films. The erosion of the films was also investigated in this study as shown in Fig. 6b. The erosion of the thinnest films was significantly lower ($P < 0.05$) than the thicker films (88.0 and $116.5\mu\text{m}$). The water uptake and erosion of the composite films could be determined in acidic medium because silver was rapidly changed to water-insoluble alginic acid (ostberg et al., 1994) and in situ insoluble films were formed. Other media, distilled water and phosphate buffer at neutral pH, could not measure these parameters due to a rapid swelling and dissolution of the films. Increasing in water uptake of the thick films suggested that the higher water-filled channels in the matrix structure were created. This indicated that the thick films had a loosen matrix structure compared with the thin films. An erosion of the composite films took place because of dissolution of some silver on the surface of the films and some water-soluble substances of clay. The % erosion of the thick films increased because water-soluble substances could easily diffuse out of the films, which possessed loosen matrix structure. Moreover, higher erosion of the thick films was one of the reasons to explain the increase in water uptake.

Permeability of the films

The effect of film thickness on water vapor permeation (WVP) is presented in Fig. 7a. Relationship between the amount of water vapor permeated and time showed a linear line over 72 h of the test and the slope of this relationship was WVP rate.

The WVP rate significantly decreased ($P < 0.05$) with increasing film thickness (Fig. 7b). This is likely to be due to the increase in the diffusion path length of the thick films. However, the WVP rate did not represent the permeability of the films, so water vapor permeability (WVP) coefficient, calculated using Eq. (4), was used for comparison. WVP coefficient statistically increased ($P < 0.05$) with increasing film thickness as shown in Fig. 7b.

It can be seen that the different results of WVP rate and WVP coefficient were found when increasing the film thickness. This indicated that the higher water vapor permeability of the thick film was found when compared with the thin films. This also suggested the different matrix structure of the films, which the thick films had looser matrix structure than the thin films.

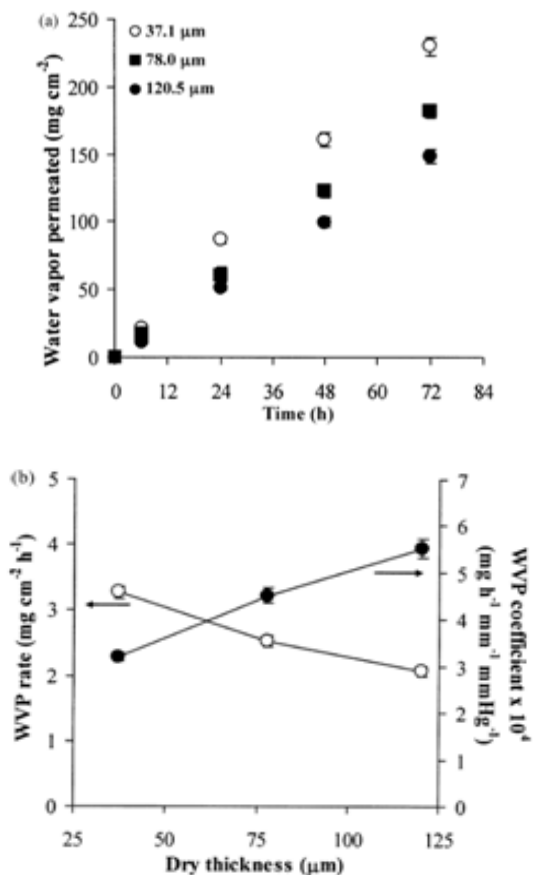


Fig. 7. Effect of dry thickness of nano composite films on water vapor permeation profiles (a), and relationship between dry thickness and WVP rate and WVP coefficient (b). Each point is the mean ± S.D., n=5.

Conclusion

The different thicknesses of the silver–clay nano composite films can be prepared by varying volumes of the composite dispersion for casting and then using solvent evaporation method for drying. The evaporation rate of solvent in different volumes used could affect crystallinity of the nano composite films and strength of the film surface and film bulk. The higher the film thickness, the weaker the film bulk was obtained. This was resulted from a loose matrix structure of the thick films. Consequently, the water uptake and erosion, as well as the water vapor permeability of the thick films were higher than those of the thin films. The findings suggest that the film thicknesses of the silver–clay nanocomposite films prepared by varying volumes of the composite dispersion for casting could influence

crystallinity, mechanical properties, water absorption and film permeability.

References

- ASTM, D 882, 2002. Standard test methods for tensile properties of thin plastic sheeting, Annual Book of ASTM Standards, vol. 06.01. ASTM International, West Conshohocken, pp. 164–173.
- Bangert, H, A. Kaminitschek, A. Wagendristel, A. Barna, P.B. Barna, G. Radnóczy, 1986, Thin Solid Films 137 -193.
- Darder, M., Colilla, M., Ruiz-Hitzky, E., 2003. Biopolymer–clay nanocomposites based on chitosan intercalated in montmorillonite. Chem. Mater. 15, 3774–3780.
- Draget, K.I., 2000. Alginates. In: Philips, G.O., Williams, P.A. (Eds.), Handbook of Hydrocolloids. Woodhead Publishing, Cambridge, pp. 379–395.
- Grim, R.E., 1953. Clay Mineralogy. McGraw-Hill Book Company, Inc., New York, pp. 190–249.
- Jansson, A., Thuvander, F., 2004. Influence of thickness on the mechanical properties for starch films. Carbohydr. Polym. 56, 499–503.
- Lagaly, G., 1999. Introduction: from clay mineral–polymer interaction to clay mineral–polymer nanocomposites. Appl. Clay. Sci. 15, 1–9.
- Li, T., Z. Huang, Z. Suo, S.P. Lacour, S. Wagner., 2004, Appl. Phys. Lett. 85 -3435.
- Limmatvapirat, S., Limmatvapirat, C., Luangtana-anan, M., Nuntanid, J., Oguchi, T., Tozuka, Y., Yamamoto, K., Puttipatkhachorn, S., 2004. Modification of physicochemical and mechanical properties of shellac by partial hydrolysis. Int. J. Pharm. 278, 41–49.
- McLean, R.J.A.A. Hussain, M. Sayer, P.J. Vincent, D.J. Hughes, T.J. Smith, Can. J. Microbiol., 1992. 39 - 895.
- Nyqvist, H., 1983. Saturated salt solutions for maintaining specified relative humidities. Int. J. Pharm. Tech. Prod. Manuf. 4, 47–48.
- Ogata, N., Kawakage, S., Ogihara, T., 1997. Poly(vinyl alcohol)–clay and poly(ethylene oxide)–clay blends prepared using water as solvent. J. Appl. Polym. Sci. 66, 573–581.
- Ostberg, T., Lund, E.M., Graffner, C., 1994. Calcium alginate matrices for oral multiple unit administration. IV. Release characteristics in different media. Int. J. Pharm. 112, 241–248.
- Pongjanyakul, T., Pripem, A., Puttipatkhachorn, S., 2005a. Influence of magnesium aluminium silicate on rheological, release and permeation characteristics of diclofenac sodium aqueous gels in vitro. J. Pharm. Pharmacol. 57, 429–434.
- Pongjanyakul, T., Pripem, A., Puttipatkhachorn, S., 2005b. Investigation of novel alginate–magnesium aluminum silicate nano composite films for modified-release tablets. J. Control. Release 107, 343–356.
- Pongjanyakul, T., Puttipatkhachorn, S., 2007. Alginate–magnesium aluminum silicate films: effect of plasticizers on film properties, drug permeation and drug release from coated tablets. Int. J. Pharm. 333, 34–44.
- Porter, S.C., Ridgway, K., 1982. The permeability of enteric coatings and the dissolution rates of coated tablets. J. Pharm. Pharmacol. 34, 5–8.
- Reda, I, J. Hafner, P. Pongratz, A. Wagendristel, H. Bangert, B.K. Bhat., 1982, Phys. Status Solidi, A Appl. Res. 72 - 313.
- Remu nan-Lopez, C., Bodmeier, R., 1997. Mechanical, water uptake and permeability properties of crosslinked chitosan glutamate and alginate films. J. Control. Release 44, 215–225.

Strehle, S. S. Menzel, H. Wendrock, J. Acker, T. Gemming, K. Wetzig.,2004, *Microelectron. Eng.* 76 - 205.
Wang, S.F., Shen, L., Tong, Y.J., Chen, L., Phang, I.Y., Lim, P.Q., Liu, T.X., 2005. Biopolymer chitosan/montmorillonite

nanocomposites: preparation and characterization. *Polym. Degrad. Stab.* 90, 123–131.